HYDROLOGICAL PROCESSES
Hydrol. Process. **18**, 1467–1486 (2004)
Published online in Wiley InterScience (www.interscience.wiley.com). DOI: 10.1002/hyp.1423

Exploring streamflow response to effective rainfall across event magnitude scale

Teemu Kokkonen,[1]* Harri Koivusalo,[1] Tuomo Karvonen,[1] Barry Croke[2] and Anthony Jakeman[2]

[1] *Laboratory of Water Resources, Helsinki University of Technology, PO Box 5300, FIN-02015 HUT, Espoo, Finland*
[2] *Centre for Resource and Environmental Studies, The Australian National University, Canberra, ACT 0200, Australia*

Abstract:

Sets of flow events from four catchments were selected in order to study how dynamics in the conversion of effective rainfall into streamflow depends on the event size. The approach taken was to optimize parameters of a linear delay function and effective rainfall series concurrently from precipitation–streamflow data without imposing a functional form of the precipitation filter *a priori*. The delay function is an instantaneous unit hydrograph (IUH) having a mathematical form of the two-parameter gamma distribution. Results from two small research catchments (0·18 and 0·63 km^2) with sub-daily data suggest a clear relationship between the event magnitude and response dynamics. The effect of the sampling frequency of data was addressed by gradually increasing aggregation interval of rainfall and flow data and repeating the optimization for each aggregated dataset. IUHs for different data aggregation intervals (for a single event) tended to be similar unless the aggregation changed the locations of data peaks. IUHs identified in larger catchments (58 and 1235 km^2) also showed variability through events; however, no systematic event magnitude dependence, as was visible in the small research catchments, was detected. Finally, the dependency detected in the small catchments was exploited in a rainfall-runoff model, where the scale parameter of the gamma distribution was linearly related to the effective rainfall intensity. Prediction of peak flows improved when the event dependency was taken into account. Copyright © 2004 John Wiley & Sons, Ltd.

KEY WORDS rainfall; event magnitude; streamflow; instantaneous unit hydrograph; rainfall-runoff model

INTRODUCTION

Mathematical straightforwardness in identification of linear systems is appealing, and linear models have also been widely used in rainfall-runoff studies. However, nonlinearity inherent in the catchment hydrological response cannot be neglected when constructing runoff predictions. Literature discusses two types of nonlinearity in basin response (see Goodrich *et al.* (1997) and Sivapalan *et al.* (2002)). The classical definition of nonlinearity from systems theory refers to the case where input–output linearity via proportionality and superposition does not hold. The other definition of nonlinearity considers the dependence of a catchment hydrological statistic (e.g. mean annual runoff) on the area of the catchment. To distinguish between these two definitions, Sivapalan *et al.* (2002) proposes the term 'scaling relationship' in the context of the latter definition.

From the view of the classical (dynamical) sense of nonlinearity, the primary factor underlying nonlinearity in rainfall-runoff response is the temporal variability in the soil moisture conditions within a catchment (e.g. Todini, 1996). A common technique to account for the control of catchment moisture on the runoff generation is to apply a nonlinear pre-filter that passes the runoff-producing fraction of precipitation (i.e. effective rainfall) into a linear delay procedure. Adopting such a framework implies that nonlinearity in

* Correspondence to: Teemu Kokkonen, Laboratory of Water Resources, Helsinki University of Technology, PO Box 5300, FIN-02015 HUT, Espoo, Finland. E-mail: tkokko@water.hut.fi

Received 31 March 2002
Accepted 20 January 2003

Copyright © 2004 John Wiley & Sons, Ltd.

basin response is present merely in determining the runoff-producing fraction of rainfall conditioned on the catchment moisture status. This modelling philosophy, originally proposed by Sherman (1932) as the unit hydrograph (UH) method, has since been widely applied (e.g. Jakeman and Hornberger, 1993; Young, 2001; Cheng and Wang, 2002) and remains one of the most practical tools for quantifying rainfall–runoff relationships (ASCE, 1996; Boufadel, 1998).

The UH is defined as the runoff response to a unit depth of effective rainfall produced by a storm of uniform intensity and specified duration. UHs can be derived either directly from rainfall-runoff records without making prior assumptions about the functional form of the UH, or indirectly by fitting a pre-selected synthetic UH against data. A UH has a specified time base, which is equal to the duration of the unit effective rainfall input. An instantaneous UH (IUH) results when the duration of the input becomes infinitesimally short. An IUH is computationally attractive, as UHs of any time base can be obtained when the functional form of the IUH is known. Nash (1957, 1959) was among the first hydrologists to suggest a parsimonious functional form, the two-parameter gamma distribution, for the IUH. One way to conceive the IUH is to consider it as a probability density function for water-particle residence times within the catchment. Following this interpretation Rodríguez-Iturbe and Valdés (1979) studied relationships between IUH parameters and catchment geomorphologic properties expressed through Horton's laws of drainage, and introduced the geomorphologic IUH (GIUH). Jakeman *et al.* (1990) and Young (2001) have used a transfer function formulation as a delay procedure between effective rainfall and streamflow. After the structure and parameters of the linear transfer function have been identified, the dynamics of the system can be depicted as a unit response function, which is equivalent to an IUH.

The traditional UH method is based on the assumption that the UH is not storm dependent, i.e. the dynamics in the conversion of effective rainfall into streamflow do not change with the event size. Several studies, however, have questioned the plausibility of not considering nonlinearity potentially present in the delay procedure (Minshall, (1960); Rodríguez-Iturbe and Valdés, 1979; Rodríguez-Iturbe *et al.*, 1982a; Blažková, 1992). Based on measurements from small catchments, Minshall 1960 showed that UH derived for one catchment may vary with the event size. This observation has been put into mathematical form, e.g. by Ding (1974) and Chen and Singh (1986), who have presented functional representations for a time-variable IUH. Rodríguez-Iturbe and Valdés (1979) attributed time variability of the GIUH to a changing flow velocity, both throughout a single storm and for different storms. The variability of the GIUH between different storms has been demonstrated by Rodríguez-Iturbe *et al.* (1979) and Georgakakos and Kabouris (1989). Gupta *et al.* (1980) suggested that the implicit assumption of linearity of the effective rainfall–streamflow transformation is questionable for small catchments. Blöschl and Sivapalan (1995) noted that nonlinearity of streamflow response increases with decreasing catchment size when the delay related to hillslope processes can no longer be neglected.

The objective of this paper is to explore how the dynamics in the conversion of effective rainfall into streamflow depends on the event size. Analysis is conducted in two stages. In the first stage, the validity of assuming a linear delay procedure (i.e. a constant IUH) is explored by analysing measured runoff events of different magnitudes through variable sampling intervals and catchments of different sizes. The effect of the event magnitude scale is studied by classifying flow events according to the peak flow and by comparing the IUHs identified separately for each event. The repetition of the comparison for catchments of different sizes and for different data aggregation intervals briefly addresses the event magnitude dependency across spatial and temporal scales respectively. The approach taken in the first stage is to estimate the IUH parameters and effective rainfall series concurrently from precipitation–streamflow data without imposing a functional form of the precipitation filter *a priori*. Similar ideas have been implemented in earlier studies (Duband *et al.*, 1993), and in this study the free calibration framework is harnessed to explore the structure of the event magnitude dependency in the IUH shape empirically for the purposes of a continuous rainfall-runoff simulation. It is noteworthy that, in the current analysis, in contrast to the precipitation filter, the functional form of the IUH must be fixed in order to have a meaningful optimization problem.

Copyright © 2004 John Wiley & Sons, Ltd.

In the second stage of the analysis, any systematic dependency identified from the data will be utilized to formulate a structure for an event-dependent IUH. Implications of nonlinearity on runoff prediction accuracy are assessed by comparing simulation results from rainfall-runoff models involving either a constant (linear) or a variable (nonlinear) IUH scheme.

SITES AND DATA

Rudbäck

Half-hourly streamflow and meteorological data were available from a small research catchment of the Finnish Environment Institute located in Siuntio, southern Finland (Rudbäck, 0·18 km^2). The catchment (Figure 1) is covered by a mature forest stand dominated by Norway spruce. Elevation ranges from 34 to 65 m above mean sea level. Bedrock is exposed on the hilltops, and soils are composed of silty and sandy moraines with an average depth of 1 to 2 m to the bedrock. More details on the site are given by Lepistö (1994) and Lepistö and Kivinen (1997).

The climate in Siuntio is temperate, with cold, wet winters, and precipitation is typically of a relatively low intensity. Approximately 30% of precipitation falls as snow. Mean annual precipitation, uncorrected for wind effects, was 700 mm during 1991–96. Mean monthly temperatures in February and July are −2 °C and 16 °C respectively.

In 1996, a measurement campaign was initiated to provide meteorological, snow and streamflow data for calibration and validation of hydrological models (Kokkonen *et al*., 2001; Koivusalo and Kokkonen, 2002). The data from 1996 to 2001 include hourly records of precipitation and streamflow.

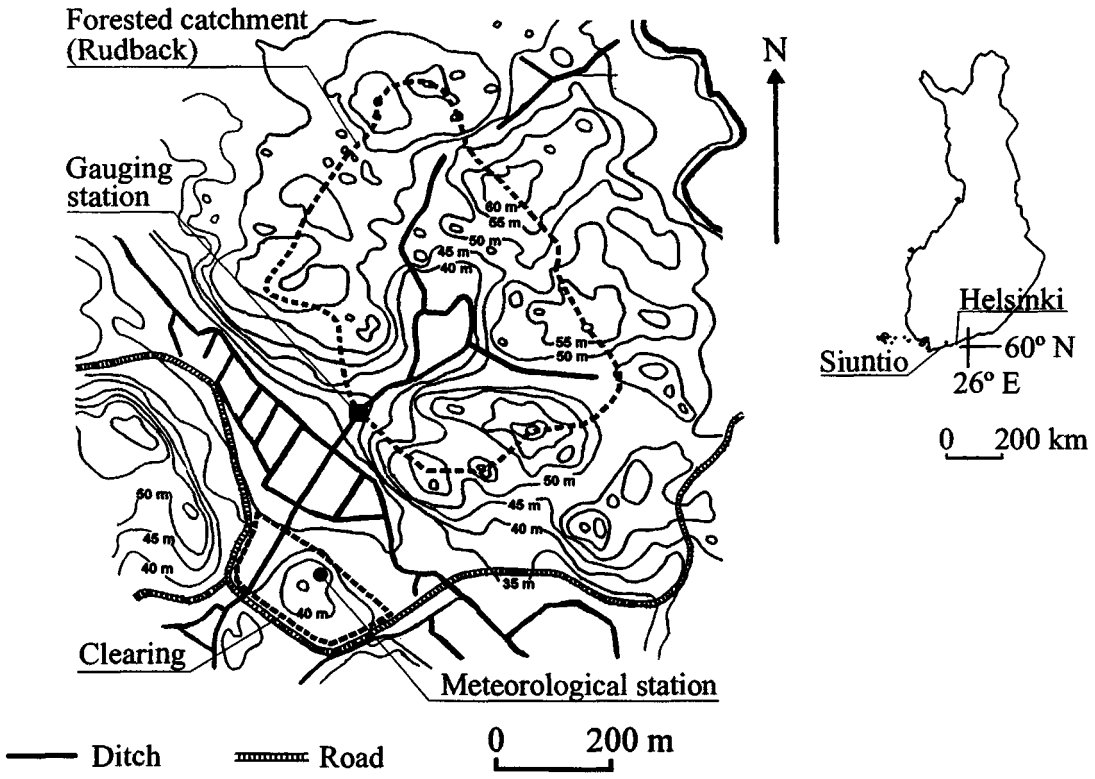

Figure 1. Rudbäck catchment in Siuntio in southern Finland

Copyright © 2004 John Wiley & Sons, Ltd.

Andrews Watershed 2

Andrews Watershed 2(0·63 km^2) is one of the research catcments in the H. J. Andrews Experimental Forest, Oregon, USA. Watershed 2 (Figure 2) is completely forested with Douglas fir and western hemlock as the dominating tree species. Elevation within the catchment ranges from 548 to 1070 m, and soils are predominantly composed of loams and clay loams. Depth to the weathered parent material is usually over 1 m. A more detailed description of the H. J. Andrews Experimental Forest can be found in Van Cleve and Martin (1991).

The climate is maritime, with wet, mild winters and dry, cool summers. The mean monthly temperature ranges from 1 °C in January to 18 °C in July. Average annual precipitation varies with elevation, from about 2300 mm at the base to over 3550 mm at upper elevations, falling mainly in November through to March. Rain predominates at low elevations; snowfall is more common at higher elevations. The highest streamflow occurs generally in November through to February, during rain-on-snow events.

Quarter-hourly streamflow and precipitation measurements, and daily minimum and maximum air temperature values, were available from the catchment. Precipitation, streamflow, and temperature data covered the period from 1958 to 1990. In addition, snow depth and meteorological data (November 1997–May 1999) from the central climatic station at an elevation of 1017 m were used in the calibration of a snow model.

Vantaanjoki basin, Finland

The Finnish Environment Institute provided daily streamflow records from two sub-catchments of the Vantaanjoki basin (Figure 3), a 58 km^2 catchment gauged at Santamäki and a 1235 km^2 catchment gauged at Myllymäki. The streamflow data covered the periods from 1971 to 1995 and from 1961 to 2001 for Santamäki and Myllymäki respectively. Land use in the Vantaanjoki basin comprises forest (46%), agricultural land (29%), urban areas (12%), peat land (9%), and open water bodies (3·5%). Urban areas are concentrated in the south, and the fraction of forest-covered area increases towards the north. Forests are mainly scattered in the landscape as isolated patches. The elevation within the basin ranges from sea level up to 135 m. Santamäki station is located at the elevation of 43 m and Myllymäki station is just above sea level. The Salpausselkä ridge runs from southeast to northwest and divides the basin into two regions. Large depositions of sand and gravel are found in the ridge area, sand and moraine soils predominate north of the ridge, and fine-grained materials are dominant south of the ridge. The climate south of the Salpausselkä ridge is similar to that of Siuntio, and north of the ridge it has a slightly more continental character. HWED (1994) provides a more detailed discussion on the Vantaanjoki area.

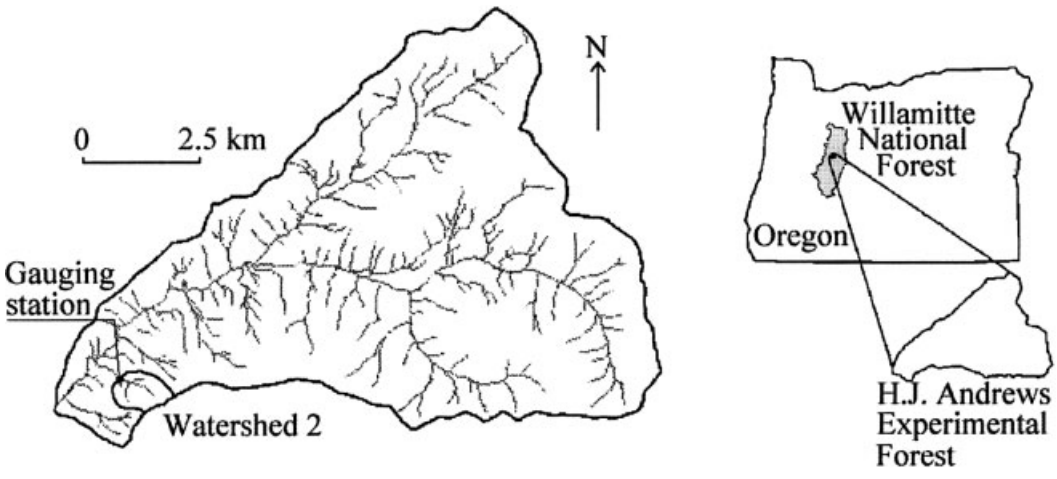

Figure 2. Watershed 2 in Andrews Experimental Forest, Oregon, USA

Copyright © 2004 John Wiley & Sons, Ltd.

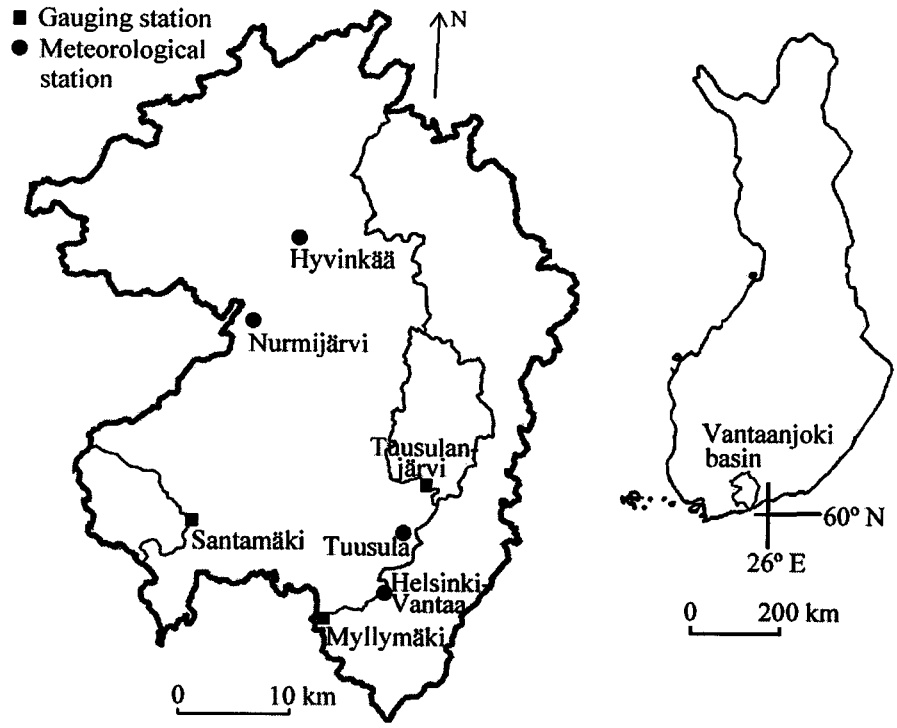

Figure 3. Vantaanjoki basin in southern Finland. Meteorological station in Helsinki–Vantaa airport, Nurmijärvi, Tuusula, and Hyvinkää are also shown

Precipitation and air-temperature data were taken from meteorological stations operated by the Finnish Meteorological Institute (Figure 3). For the Santamäki catchment the data were from Nurmijärvi, which is located 14 km from the gauging station. Areal values of precipitation and air temperature for the Myllymäki catchment were computed with the Thiessen method using point data from four stations (Helsinki–Vantaa airport, Nurmijärvi, Tuusula, Hyvinkää) located within the catchment (Figure 3). Areal estimates of the snow water equivalent were based on snow-course measurements from Tuusulanjärvi sub-catchment (Figure 3).

METHODS

Conversion of effective rainfall into streamflow

The time convolution of effective rainfall u with an IUH determines streamflow Q as

$$Q(t) = \int_0^t \mathrm{IUH}(t-s)u(s)\mathrm{d}s \tag{1}$$

where t is time. A gamma distribution has a classical shape of an idealized IUH, in having both rise and recession limbs, and it has been extensively applied in rainfall-runoff studies (e.g. Aron and White, 1982; Rosso, 1984; Boufadel, 1998). The performance of the gamma distribution as an IUH has also received criticism (Duband *et al*., (1993)), particularly in regard to problems replicating sharply peaked UHs (Boufadel, 1998). Yet, it was deemed to be suitable as a delay function for the purposes of the current study. The IUH formulated as the two-parameter gamma distribution reads

$$\mathrm{IUH}(t) = \frac{1}{\beta^{\alpha}\Gamma(\alpha)} t^{\alpha-1}\, \mathrm{e}^{-t/\beta} \qquad \alpha \geq 1, \beta > 0 \tag{2}$$

Copyright © 2004 John Wiley & Sons, Ltd.

where α is the shape parameter, β is the scale parameter, and Γ is the gamma function. The 1 h UHs were computed via numerical integration of IUH(t) in segments having a length of 1/100 h. In time convolutions, the 1 h UH was always used. Whenever the data discretization was coarser, the data were distributed uniformly into 1 h intervals.

In addition to the parameters α and β, the following IUH characteristics are reported in the Results and discussion section. Time to the IUH peak t_p is computed from

$$t_p = (\alpha - 1)\beta \tag{3}$$

and the magnitude of the IUH peak IUH_{max} is derived from

$$IUH_{max} = IUH(t_p) \tag{4}$$

and the time to a 20% mass throughput $t_{20\%}$ is solved from

$$0{\cdot}2 = \int_0^{t_{20\%}} IUH(t)dt \tag{5}$$

Derivation of effective rainfall

Most commonly, effective rainfall is defined as the portion of rainfall that generates direct or surface runoff (e.g. Garklavs and Oberg, 1986; Pilgrim and Cordery, 1992; Wang *et al*., 1992). In other words, effective rainfall is that part of the rainfall that is not lost to infiltration, depression storage, and interception. As infiltration is regarded to be a loss, the baseflow contribution to the total flow hydrograph needs to be separated out first. Closely related to the above definition, effective rainfall can also mean the share of precipitation that eventually emerges as streamflow regardless of the runoff transport mechanism (e.g. Jakeman and Hornberger, 1993). This definition contrasts with the most common one, in that (1) infiltration is no longer considered to be an abstraction and infiltrated water can also contribute to streamflow, and (2) in addition to interception, evapotranspiration also contributes to losses.

In the first stage of the study, where the event magnitude dependency of the IUH is explored, the determination of the effective rainfall is based on the methodology presented by Duband *et al*. (1993). The idea is to allow the effective rainfall time series to have any plausible values and then to choose them in such a manner that the subsequent convolution with the IUH reproduces the best possible match to the measured streamflow. Some restrictions on the effective rainfall need to be imposed, because it is easy to demonstrate that, otherwise, for any arbitrary UH an input can always be found so that the measured output is fitted exactly (Nalbantis *et al*., 1995). Following Duband *et al*. (1993), the effective rainfall is taken as a fraction of the measured rainfall and it is not allowed to exceed the measured rainfall at any time step. Gamma distribution parameters α and β and effective rainfall time series were optimized concurrently for each event separately. Events should preferably have a negligible initial flow. Since such events, especially those with a high peak flow, are rare, one needs to take into account the effect of a nonzero initial flow. Recession of initial flow was estimated from the flow data by fitting an exponential decay function to observed flow recession data (Figure 4). Initial flow and its recession account for the effect of rainfalls prior to the study period.

In the second stage of the study the event magnitude dependency of the IUH is implemented into a continuous rainfall-runoff simulation model. The complete model comprises a loss module, to generate effective rainfall from climatic input, and an event-dependent IUH, whose structure is formulated on the basis of the results from the first stage. The loss module, which is based on the catchment moisture deficit model of Evans and Jakeman (1998), uses two constant multipliers (c, e) and a threshold (d) to derive an estimate that characterizes evapotranspirational losses E as a function of the air temperature T and the moisture deficit D. In mathematical terms:

$$\left\{ \begin{array}{ll} E = cT & D \le d \\ E = cT\exp[e(1 - D/d)] & D > d \end{array} \right\} \tag{6}$$

Copyright © 2004 John Wiley & Sons, Ltd.

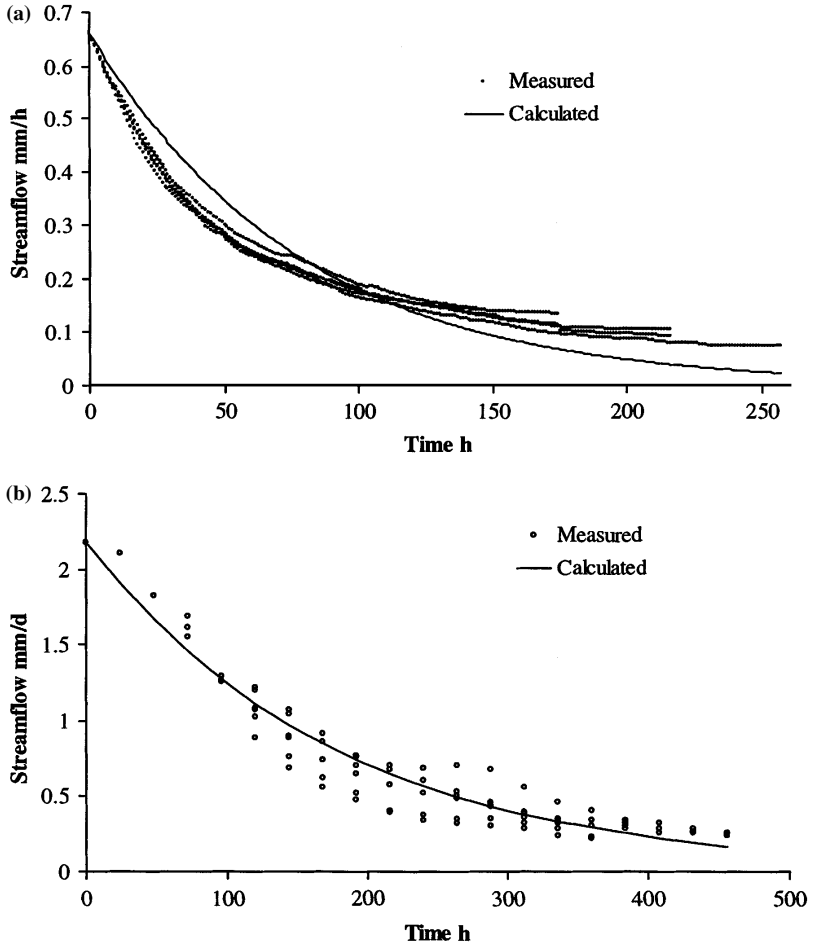

Figure 4. Estimation of initial flow recession against measured hourly data from (a) Andrews Watershed 2 and (b) measured daily data from Myllymäki

The effective rainfall U is computed from the observed rainfall P and the moisture deficit from the drainage equation

$$\left\{\begin{array}{ll} \mathrm{d}U/\mathrm{d}P = 1 - D/a & D \leq a \\ \mathrm{d}U/\mathrm{d}P = 0 & D > a \end{array}\right\} \tag{7}$$

where a is a threshold parameter for generation of effective rainfall.

Finally, the moisture deficit is updated using the mass balance equation

$$\frac{\mathrm{d}D}{\mathrm{d}t} = E + U - P \tag{8}$$

The four parameters of the loss module, and the initial value of the moisture deficit, are optimized against measured streamflow records.

In simulations conducted with the complete rainfall-runoff model (i.e. the loss module coupled with an IUH scheme), the initial flow at the beginning of an event is not of concern as long as the simulation is commenced well before the event of interest. Therefore, in stage 2, no separate computation for recession of

Copyright © 2004 John Wiley & Sons, Ltd.

the initial flow is carried out. Accumulation and melt of snow cover were not considered in the rainfall-runoff simulations.

All optimizations in both stages were carried out using the shuffled complex evolution method (SCE-UA) of Duan *et al.* (1992). The sum of squared error between measured and calculated streamflow was used as the objective criterion.

Event screening criteria

Precipitation–streamflow series in each catchment were screened to select a set of events that covers as large a range of peak flow values as possible. Particularly in the Finnish catchments, many of the largest flow events are often induced by snowmelt. In the case of snowmelt, the input passed through the delay function should be effective snowmelt, i.e. the fraction of melt water that contributes to streamflow. With the available snow data, however, uncertainties were deemed to be too great to construct snowmelt time series at time scales corresponding to those of the flow observations, and with an accuracy comparable to that of the precipitation input. Instead, snow simulation results were used to reject events likely to be predominantly produced by snowmelt.

When the storm event generates only little streamflow the observed rainfall does not impose a strong enough restriction on the effective rainfall, which easily leads to multiple local optima within the parameter space (IUH parameters and effective rainfall values). To avoid this, events having a low runoff coefficient, i.e. cumulative streamflow divided by cumulative precipitation, were screened out. Finally, events having an undisturbed recession with no major storms occurring after the flow peak were prioritized.

RESULTS AND DISCUSSION

Event selection

In Rudbäck, snowmelt periods were identified on the basis of the modelling results reported in Koivusalo and Kokkonen (2002), and streamflow events affected by snowmelt were disregarded accordingly. Events with a runoff coefficient lower than 20% were not accepted into the analysis. The total number of selected events in Rudbäck was nine. Total depths and maximum intensities of streamflow and rainfall, and event dates, are listed in Table I for all events. Considering the relatively short record length (5 years) in Rudbäck, the representativeness of the high-intensity storm events is limited.

Snow accumulation and melt in Andrews Watershed 2 were estimated using a simple degree-day snowmelt model, which used daily precipitation and air temperature time series as inputs. The model was calibrated

Table I. Total depths and maximum intensities of streamflow and precipitation for nine events in Rudbäck. Hours where precipitation exceeded 0·5 mm have been included into precipitation duration (precipitation hours)

Event	Start	Duration (h)	Precipitation hours (h)	Total precipitation (mm)	Total flow (mm)	Maximum precipitation (mm h^{-1})	Maximum flow (mm h^{-1})
1	22 Aug 1998 00:00	148	10	22	14	7·13	0·23
2	14 Oct 1998 13:00	71	11	15	5	2·47	0·14
3	17 Oct 1998 16:00	68	16	28	11	4·96	0·28
4	28 Oct 1998 07:00	105	28	51	42	6·56	0·88
5	30 Nov 1999 21:00	78	7	21	8	4·71	0·20
6	30 Oct 2000 12:00	79	18	27	11	3·93	0·25
7	5 Nov 2000 11:00	75	17	42	35	6·61	1·40
8	13 Nov 2000 17:00	113	18	29	25	5·01	0·51
9	18 Nov 2000 12:00	98	12	20	14	2·43	0·27

Copyright © 2004 John Wiley & Sons, Ltd.

against snow depth data (November 1997 to May 1999) available from the central meteorological station. The Nash and Sutcliffe (1970) efficiency for the model fit was 0·91. The calibrated snow model was then used to simulate snow water equivalent in Watershed 2 with meteorological input measured next to the catchment. Many of the highest streamflow peaks in Watershed 2 occurred during rain-on-snow conditions. Such events could be selected when they had clearly higher rainfall intensities compared with predicted snowmelt intensities. Precipitation and streamflow characteristics for the selected 17 events are presented in Table II.

In the Santamäki and Myllymäki catchments, the degree-day model was again used for revealing periods of snowmelt. The model was calibrated against areal snow water equivalent from Tuusulanjärvi catchment for a period from 1961 to 2001. The Nash and Sutcliffe efficiency for the model fit was 0·91. Subsequently, the model was applied to Santamäki and Myllymäki catchments with the precipitation and air temperature inputs presented earlier. Event characteristics for 13 events in Santamäki and 21 events in Myllymäki are shown in Table III and Table IV respectively.

Effect of event magnitude scale

The relationship between the event magnitude and the identified IUH is studied first using data from the small catchments of Rudbäck (0·18 km^2) and Andrews Watershed 2 (0·63 km^2).

The selected data time-steps were 1 h for Rudbäck and 2 h for Andrews Watershed 2. Shorter time intervals were not included into the analysis in order to constrain the number of effective rainfall values to be optimized. The rationale for the longer time step in Andrews lies in its wet, maritime climate giving rise to a greater number of rainy days than there are in Rudbäck. Figure 5 shows the estimated IUHs for nine events in Rudbäck and 17 events in Andrews Watershed 2. IUHs are plotted in descending order of the measured event peak flows, and it is easy to detect that streamflow events of greater magnitude tend to have a flashier response in both catchments.

Model optimization using the SCE-UA method was successful and yielded IUH parameters and a series of effective rainfall that reproduced the measured streamflows very well. The average Nash–Sutcliffe efficiencies

Table II. Total depths and maximum intensities of streamflow and precipitation for 17 events in Andrews Watershed 2. Hours where precipitation exceeded 0·5 mm have been included into precipitation duration (precipitation hours)

Event	Start	Duration (h)	Precipitation hours (h)	Total precipitation (mm)	Total flow (mm)	Maximum precipitation (mm h^{-1})	Maximum flow (mm h^{-1})
1	3 Dec 1968 08:00	109	38	133	131	7·92	3·22
2	4 Dec 1971 16:00	85	36	127	104	9·05	2·72
3	1 Mar 1972 13:00	108	43	164	156	7·27	3·21
4	4 Mar 1974 14:00	109	34	87	65	6·08	1·10
5	27 Feb 1975 08:00	61	25	69	41	5·69	0·87
6	23 Mar 1975 12:00	133	36	73	78	3·84	1·09
7	23 Dec 1977 10:00	135	32	68	82	4·12	1·03
8	2 Feb 1978 12:00	109	23	75	61	6·35	1·01
9	5 Dec 1981 02:00	109	42	163	130	8·49	3·32
10	13 Dec 1981 10:00	109	55	177	124	7·39	2·05
11	12 Feb 1984 06:00	133	57	211	156	7·64	3·56
12	26 Nov 1986 10:00	99	45	108	89	5·23	1·51
13	27 Nov 1988 08:00	111	21	59	67	5·08	1·15
14	8 Jan 1989 16:00	107	43	154	121	8·96	3·68
15	27 Apr 1990 00:00	85	34	135	73	9·31	2·08
16	25 Nov 1991 01:00	104	45	124	86	8·36	1·51
17	5 Dec 1991 15:00	109	36	121	82	5·59	1·50

Copyright © 2004 John Wiley & Sons, Ltd.

Table III. Total depths and maximum intensities of streamflow and precipitation for 13 events in Santamäki. Days where precipitation exceeded 0·5 mm have been included into precipitation duration (precipitation days)

Event	Start	Duration (days)	Precipitation days (days)	Total precipitation (mm)	Total flow (mm)	Maximum precipitation (mm day^{-1})	Maximum flow (mm day^{-1})
1	25 Aug 1972	10	6	66	15	37·8	3·5
2	27 Sep 1973	13	8	57	18	24·0	3·9
3	9 Nov 1974	16	9	50	44	9·8	4·2
4	30 Aug 1981	21	8	48	22	17·2	2·4
5	18 Oct 1984	21	12	121	41	36·1	3·5
6	4 Nov 1985	26	12	68	32	16·0	3·4
7	19 Oct 1986	10	4	46	18	18·7	4·2
8	22 Nov 1986	10	7	53	29	22·5	6·6
9	23 Sep 1987	14	5	38	19	24·7	4·0
10	3 May 1988	16	2	9	16	8·2	2·9
11	6 Oct 1988	17	4	36	18	14·0	3·5
12	9 Oct 1993	14	5	45	9	18·5	2·1
13	2 Oct 1994	9	5	29	10	18·8	2·6

Table IV. Total depths and maximum intensities of streamflow and precipitation for 21 events in Myllymäki. Days where precipitation exceeded 0·5 mm have been included into precipitation duration (precipitation days)

Event	Start	Duration (days)	Precipitation days (days)	Total precipitation (mm)	Total flow (mm)	Maximum Precipitation (mm day^{-1})	Maximum flow (mm day^{-1})
1	5 Sep 1962	28	13	134	97	56·2	7·9
2	31 Oct 1962	13	3	22	25	12·3	3·4
3	11 May 1964	27	7	27	26	7·3	3·5
4	29 Oct 1965	27	11	51	30	17·1	4·5
5	10 May 1968	27	9	63	40	18·0	4·1
6	17 Oct 1970	21	10	95	26	34·0	5·0
7	23 Aug 1972	23	11	68	34	22·6	4·0
8	22 Jul 1979	23	9	38	24	11·6	2·5
9	22 May 1980	19	5	41	17	13·2	2·5
10	25 Aug 1981	19	9	66	44	18·9	4·0
11	15 Nov 1982	25	15	94	49	16·7	4·4
12	10 Oct 1985	17	5	24	13	8·3	1·4
13	1 Nov 1985	22	11	81	42	16·2	4·2
14	11 May 1987	21	7	38	26	12·6	3·0
15	5 Aug 1987	11	5	53	9	40·0	1·7
16	23 Sep 1987	16	8	49	34	28·2	5·5
17	6 Oct 1988	22	7	62	30	23·2	4·4
18	9 Oct 1993	22	7	44	18	22·1	2·9
19	2 Jul 1996	24	14	135	57	50·1	6·3
20	9 Nov 1997	14	3	26	12	12·7	1·5
21	4 May 1998	19	3	33	30	20·8	4·4

were 0·97 and 0·99 for Rudbäck and Andrews Watershed 2 respectively. The maximum number of optimized parameters was 38 for Rudbäck (event 4) and 48 for Andrews Watershed 2 (event 11). The numbers of flow data points were 105 and 67 for these events. It could be expected that a model with such a large number of calibration parameters would yield a good fit to the measured data. Regardless of the fact that all values of

Copyright © 2004 John Wiley & Sons, Ltd.

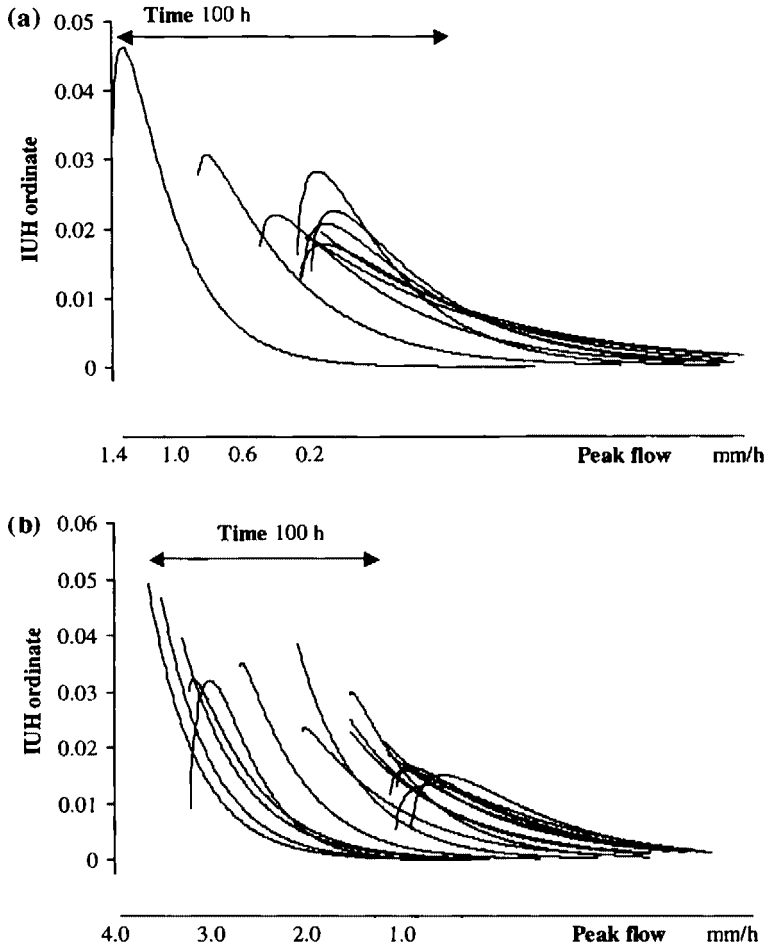

Figure 5. Estimated IUHs for (a) nine events in Rudbäck and (b) 17 events in Andrews Watershed 2. IUHs are plotted in descending order of peak flow

effective rainfall were optimized, the only constraint being that they may not be greater than the actual rainfall, a clear relationship between the IUHs and the event magnitude emerged. This relationship was quantified in terms of correlation values between IUH characteristics and the event peak flow (Table V).

IUH_{max} and $t_{20\%}$ exhibit a distinct correlation with the measured peak flow in both catchments, whereas the correlation between the peak flow and t_p is negligible. According to the empirical results of Minshall (1960) and the geomorphoclimatic theory of the IUH (Rodríguez-Iturbe *et al.*, 1982a,b), both t_p and IUH_{max} show a relation to the effective rainfall intensity. Absence of correlation between the event magnitude and t_p in Table V may not be surprising, as the runoff response to a storm is fast throughout the events in the small catchments studied. In fact, eight out of 17 IUHs identified for Andrews Watershed 2 have α parameter values equal to 1·00, implying that the IUH has the form of an exponential distribution and a t_p value of zero. The scale parameter β has a much stronger correlation with the event magnitude than α. This finding can be given a physical meaning in the light of Rosso (1984), who related α merely to catchment properties and β both to catchment properties and the streamflow velocity. Rodríguez-Iturbe (1993) proposed a relationship between the streamflow velocity and the effective rainfall intensity. By combining the ideas of Rosso (1984) and Rodríguez-Iturbe (1993), a dependence between effective rainfall and the β parameter can be expected. This,

Copyright © 2004 John Wiley & Sons, Ltd.

indeed, is the case for the present results. The correlation between the maximum intensity of the optimized effective rainfall and the β parameter is $-0{\cdot}65$ for Rudbäck (1 h data) and $-0{\cdot}78$ for Andrews Watershed 2 (2 h data), which are of the same magnitude as the correlations with the peak flow (see Table V). The peak flow, being a measured quantity, was preferred as the index of the event size in the first stage of the study.

Finally, the optimized effective rainfall series were examined. In Figure 6a, which plots rainfall, effective rainfall, and streamflow series for event 7 in Rudbäck, the fraction of precipitation converted into effective rainfall increases with time towards the flow peak. The dynamics of the runoff-producing fraction of precipitation in this event is typical for the majority of the events. Occasionally, optimization yields series of effective rainfall that are not in line with hydrological perceptions of how runoff is generated. This is evident from Figure 6b, where the effective rainfall oscillates wildly at the beginning of the event and the runoff-producing fraction of rainfall becomes zero at the time of the flow peak. Considering the large number of optimized effective rainfall values, such optimization artefacts can be expected.

Effect of sampling frequency of data

This section will explore whether the relationship identified between event magnitude and streamflow response to effective rainfall persists when the data discretization interval is gradually increased. Optimizations were carried out by aggregating the data into time intervals of 1, 3, 6, 12, and 24 h in Rudbäck, and 2, 3, 6, 12, and 24 h in Andrews Watershed 2. Event length was just a few days in these small catchments, which did not justify aggregation of data into time intervals longer than 24 h. It should be noted that, even when restricting the maximum time interval to 24 h, none of the events has more than seven flow observations remaining. This may lead to too few data points relative to the number of parameters for the optimization results to be meaningful. When there are too few data points relative to the number of parameters the optimization results may be indiscriminate, even with the constraint applied to the effective rainfall. In this section, an IUH for a t-hourly data refers to an IUH that has been optimized using a data set of a t h interval.

Examination of correlations between event size and IUH characteristics (Table V) reveals that the measured peak flow has a clear, albeit a weakening, correlation with the IUH (t_p) and the $t_{20\%}$ in both catchments. In Siuntio, no significant correlations can be found at the 24 h interval. The dependence of the parameter β on the peak flow is more distinct in Andrews Watershed 2 than in Rudbäck.

Next, we studied how the optimized IUHs behave for a single event when the time step is gradually increased. Two events, where the general IUH behaviour with increasing time step was particularly visible, were examined more closely. Figure 7 shows optimized IUHs and measured streamflow series for event 10

Table V. Correlations between IUH characteristics (α, β, t_p, IUH_{max}, $t_{20\%}$) and the event peak flow in Rudbäck and Andrews Watershed 2 for different data aggregation intervals Δt. Statistically significant correlations (at the 0·05 risk level) are given in bold

Δt (h)	α	β	t_p	IUH (t_p)	$t_{20\%}$
Rudbäck					
1	0·23	−0·66	−0·16	**0·92**	**−0·88**
3	0·27	**−0·67**	**−0·09**	**0·90**	**−0·84**
6	0·56	**−0·78**	−0·10	**0·81**	**−0·75**
12	−0·45	−0·41	−0·49	**0·89**	**−0·84**
24	−0·08	−0·23	−0·04	0·32	−0·32
Andrews Watershed 2					
2	−0·09	**−0·85**	−0·38	**0·90**	**−0·82**
3	−0·01	**−0·85**	−0·34	**0·90**	**−0·80**
6	0·27	**−0·89**	−0·13	**0·83**	**−0·74**
12	0·47	**−0·82**	0·18	**0·70**	**−0·49**
24	**0·61**	**−0·86**	0·04	**0·58**	−0·40

Copyright © 2004 John Wiley & Sons, Ltd.

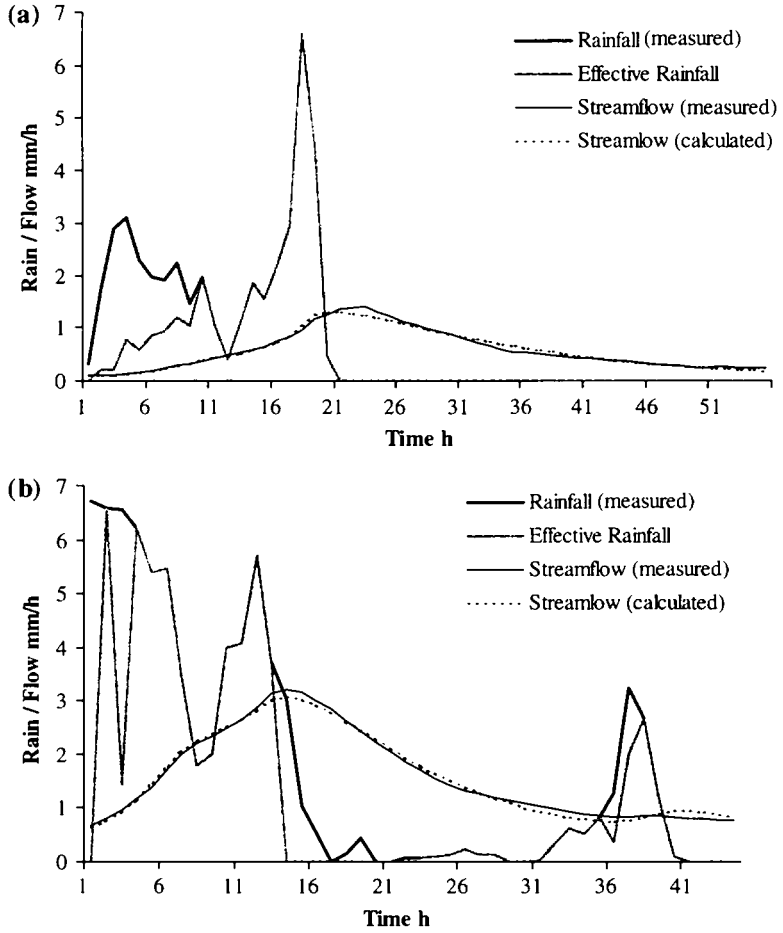

Figure 6. Rainfall, effective rainfall, and measured and computed streamflow series for (a) event 7 in Rudbäck and (b) for event 3 in Andrews Watershed 2

and event 9 in Andrews Watershed 2. For event 10, all IUHs are nearly identical, whereas in the case of event 9 the IUH for the 24 h data is notably different from the other IUHs. When looking at measured flows at different temporal discretizations, it is evident that, for the 24 h data in event 9, both the flow peak and the IUH have moved forward. A shift of the IUH peak with changing temporal discretization of the data will depend on how the aggregation influences the occurrence times of rainfall and streamflow peaks. When the length of the time step increases, the distance between rainfall and streamflow peaks depends on the distribution of rainfall and streamflow within a time step. Consequently, even when the events are of the same magnitude, it may be impossible to identify a unique IUH when the data have a coarse temporal discretization.

Effect of catchment size

In operational rainfall-runoff modelling, catchments tend to be much larger than those studied in the previous subsections. Also, the observation frequency is seldom more than 1 day. In this section, the effect of the spatial scale on the event magnitude–IUH relationship is briefly addressed by repeating the above analysis using daily data from two considerably larger catchments. Figure 8a shows identified IUHs for the Santamäki catchment (58 km^2), and Figure 8b presents them for the Myllymäki catchment (1235 km^2). The results are similar for both catchments, with no evidence of a systematic dependence between IUH characteristics and event size

Copyright © 2004 John Wiley & Sons, Ltd.

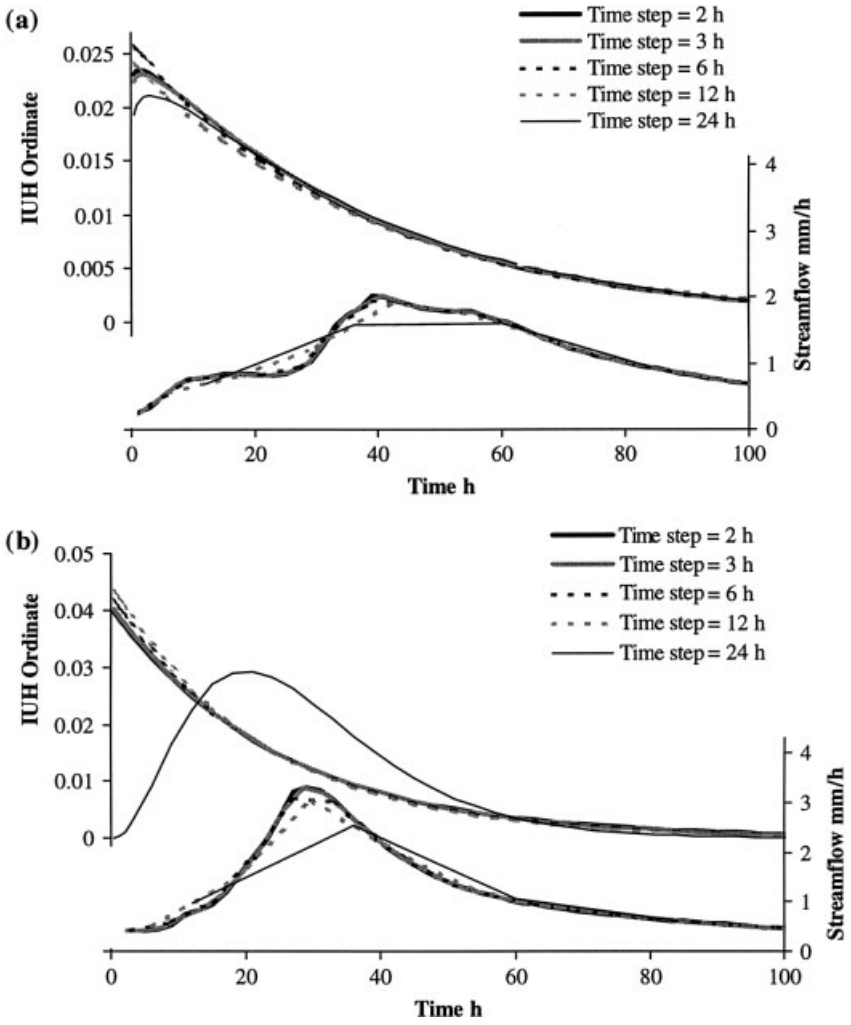

Figure 7. Optimized IUHs and measured streamflow series for (a) event 10 and (b) event 9 in Andrews Watershed 2

(Figure 8 and Table VI). Although no systematic relationship between the IUH shape and the event magnitude is present, the IUHs identified for separate events are quite varied. Potential sources for the variability of IUHs through events include nonuniform distribution of rainfall, uncertainties in estimating rainfall losses, and inaccuracies in the rainfall-runoff data. Blažková (1992) found that nonuniform spatial distribution of rainfall had a significant effect on the shape of the response in a catchment having an area of 103·4 km^2. Numerical simulations of Robinson *et al*. (1995) indicated that nonlinearity in the catchment response, arising from both hillslope properties and channel network geomorphology, does not really disappear at any spatial scale. Based on rainfall-runoff simulations in a semi-arid environment in Arizona, USA, Goodrich *et al*. (1997) suggested that nonlinearity in the catchment response with respect to peak discharge actually increased with catchment size. In their ephemeral catchments, they attributed the response becoming more nonlinear to the increasing role of channel losses and the continual decline of fractional storm area coverage. Clearly, in order to tackle the problem of the nonlinear response in large catchments, other causes of variability in catchment response than just the event magnitude should be analysed. Furthermore, hydrometeorological data from a greater number of catchments than used in this study would be required for such analysis.

Copyright © 2004 John Wiley & Sons, Ltd.

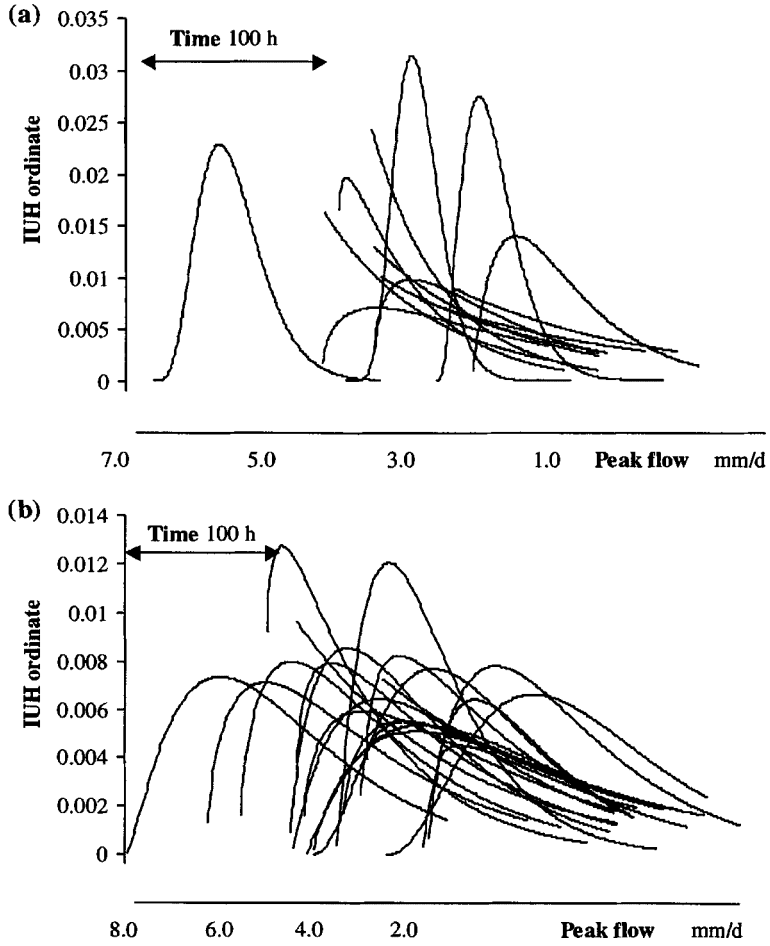

Figure 8. Estimated IUHs for (a) 13 events in Santamäki and (b) 20 events in Myllymäki. IUHs are plotted in descending order of peak flow

Table VI. Correlations between IUH characteristics (α, β, t_p, IUH_{max}, $t_{20\%}$) and the event peak flow in Santamäki and Myllymäki

Δt (days)	α	β	t_p	IUH (t_p)	$t_{20\%}$
Santamäki					
1	0·36	−0·35	0·38	0·26	0·20
Myllymäki					
1	0·05	−0·37	0·04	0·24	−0·14

Simulations with the complete rainfall-runoff model

In the previous subsections, a relationship between event magnitude and IUH parameterization was detected in the small catchments. This relationship is now used to formulate a structure for an event-dependent (variable) IUH in Andrews Watershed 2. Following the results presented earlier, the shape parameter α was fixed to a constant value of 1·12 (average value across all events using 2 h data), and the scale parameter β was related

Copyright © 2004 John Wiley & Sons, Ltd.

to the value of effective rainfall via the following linear equation:

$$\beta_k = x_1 + x_2 U_k \tag{9}$$

where x_1 and x_2 are parameters, and subscript k is the index of a computation time step. Effective rainfall U is generated with the loss module presented in the Methods section. Parameters of the loss module (*a, c, d, e*), initial value of the moisture deficit D_0, and parameters x_1 and x_2 were calibrated against measured streamflow from 1 May until 30 December 1981. Also, in order to assess the performance of the event-magnitude-dependent IUH scheme, the loss module coupled with a constant IUH scheme was calibrated against the same period of streamflow data.

The model results are compared in terms of the Nash and Sutcliffe efficiency and the prediction error at the time of measured peak flow. Table VII lists calibrated values for the model parameters and D_0, Nash and Sutcliffe efficiencies (NS), and the peak flow prediction errors $E_{q\max}$ both for the variable- and constant-IUH models. Time series of measured and computed streamflows are plotted in Figure 9. In terms of the efficiencies, both models yield good overall fits to the observed data, but the constant-IUH scheme appears to have problems reproducing the highest flow of the record occurring on 6 December.

On the basis of one underpredicted peak flow during calibration, it is not possible to discriminate between the models. Potential causes for the failure to reproduce a single event include data errors and disregard of snow processes in the model structure. The capability of the models to reproduce high flows was further assessed by validating both models to four events from Andrews Watershed 2 where the measured peak flow exceeded 3 mm h^{-1} (events 1, 3, 11, and 14). In validation mode, only the initial value of the moisture deficit at the beginning of the simulation was calibrated. The results presented in Table VII and Figure 10 show that, in three out of the four validation events (events 1, 11, and 14), the variable-IUH scheme provides a more accurate prediction of the flow peak. This is in line with the results of Chen and Singh (1986), who reported that introduction of a variable-IUH scheme improved peak discharge predictions in two catchments (17·1 and 656 km^2) in China. In the light of the present results, the variable IUH also improves model performance during recessions, particularly in events 11 and 14.

Effective rainfall fractions from the optimization (stage one), and fractions yielded by the loss module (stage two), are plotted for the validation event 14 in Figure 11. The optimized effective rainfall fraction starts low at the beginning of the event and rapidly reaches a value of unity. Both modelled fractions show a similar behaviour but exhibit much less variation, particularly the fraction from the model with a variable-IUH scheme. Less dynamical behaviour of the modelled effective rainfall fraction can be attributed to the fact that

Table VII. Parameter values and performance statistics for the complete rainfall-runoff model (with either a variable- or a constant-IUH scheme). NS denotes the Nash and Sutcliffe (1970) efficiency, and $E_{q\max}$ the flow prediction error at the time of measured maximum flow. Negative $E_{q\max}$ indicates underprediction of peak flow

Period	*a*	*c*	*d*	*e*	D_0	x_1	x_2	NS	$E_{q\max}$ (%)
Variable IUH									
Calibration	306	0·083	67·4	0·724	167	69	9.75	0·97	−2
Event 1	306	0·083	67·4	0·724	57	69	9.75	0·9	−24
Event 3	306	0·083	67·4	0·724	113	69	9.75	0·79	−26
Event 11	306	0·083	67·4	0·724	86	69	9.75	0·93	−12
Event 14	306	0·083	67·4	0·724	125	69	9.75	0·91	−13
Constant IUH									
Calibration	96.7	0·088	69·8	4·98	12·1	1.01	34	0·94	−27
Event 1	96.7	0·088	69·8	4·98	6·1	1.01	34	0·86	−27
Event 3	96.7	0·088	69·8	4·98	25·7	1.01	34	0·85	−20
Event 11	96.7	0·088	69·8	4·98	40·4	1.01	34	0·83	−24
Event 14	96.7	0·088	69·8	4·98	41·7	1.01	34	0·79	−34

Copyright © 2004 John Wiley & Sons, Ltd.

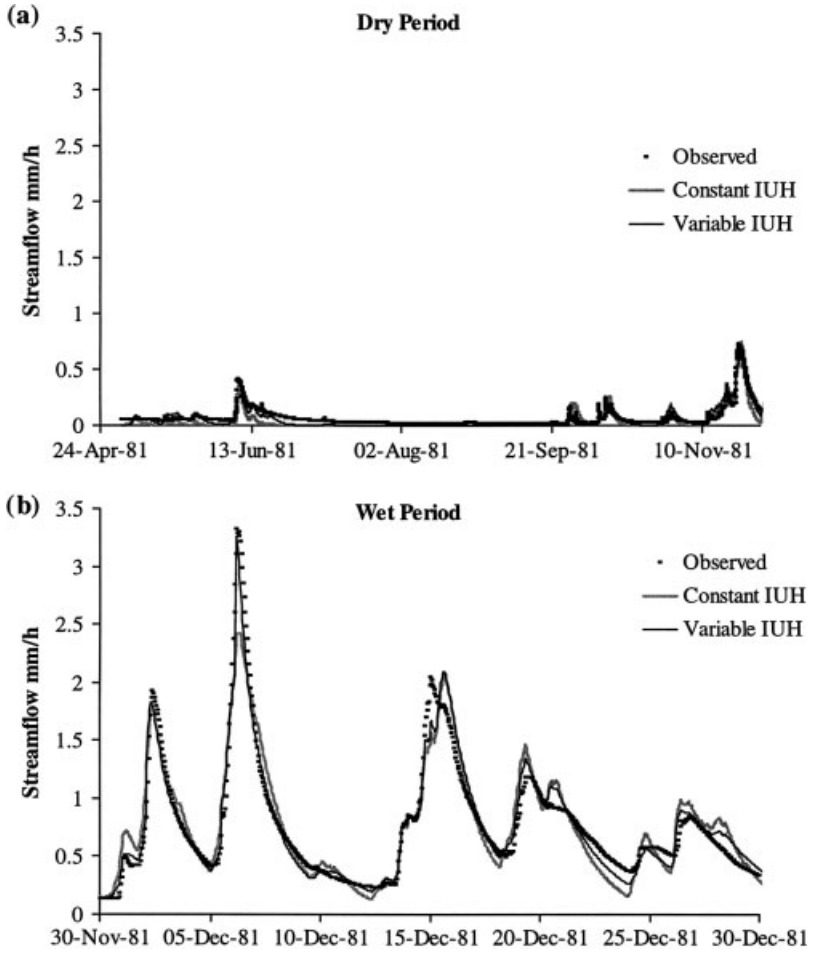

Figure 9. Observed and computed streamflows for the complete rainfall runoff model (with either a variable- or a constant-IUH scheme) for the calibration period in Andrews Watershed 2. For the sake of clarity, the period is split into two parts: (a) dry period and (b) wet period

the model was calibrated over dry and wet seasons comprising several rainfall events. It is more critical for the loss module to account for seasonal dynamics in the catchment soil moisture status than to consider short-term variation within a single event.

CONCLUSIONS

Analysis of precipitation and streamflow records revealed a clear relationship between response dynamics and event magnitude in two small research catchments. The response becomes flashier with increasing event magnitude, which is seen as a strong dependence between event size and IUH characteristics. The fact that such a relationship emerged, eventhough the effective rainfall series was optimized to allow it to take any plausible value, gives credence to this finding. The relationship between response dynamics and event magnitude weakened with an increasing data aggregation interval. When looking at single events at different temporal discretizations, the optimization generally yields similar IUHs unless the data aggregation changes the location of the peaks. The effect of the spatial scale on the event dependence of the IUH was studied briefly by using daily data from two larger catchments (58 and 1235 km^2). Systematic behaviour between the empirically

Copyright © 2004 John Wiley & Sons, Ltd.

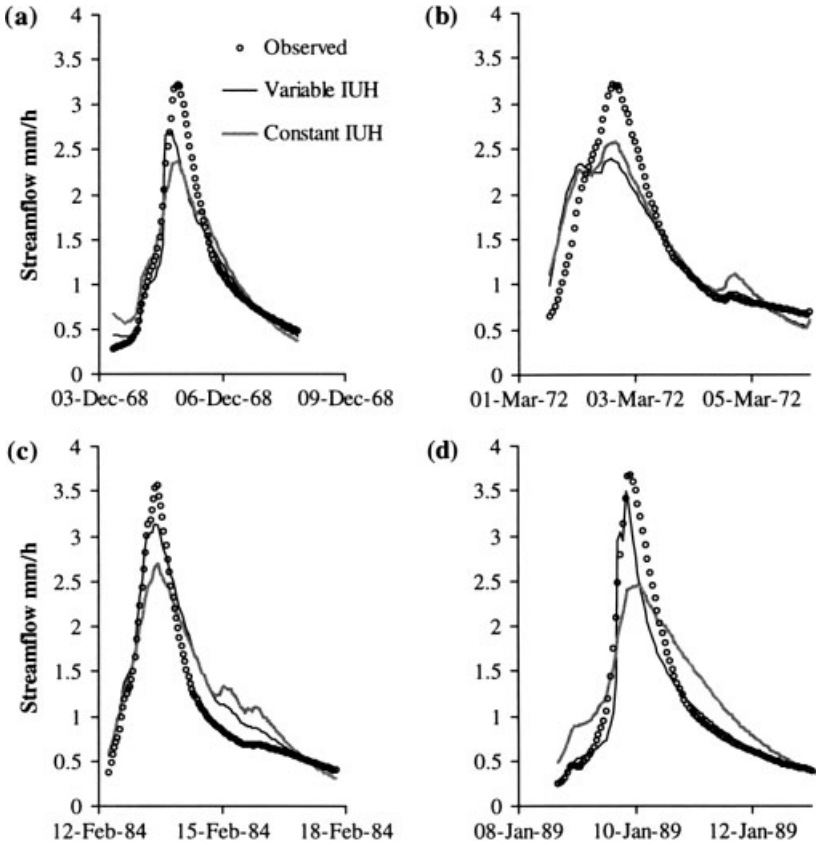

Figure 10. Observed and computed streamflows for the complete rainfall-runoff model (with either a variable- or a constant-IUH scheme) for the validation events in Andrews Watershed 2. The events are: (a) event 1, (b) event 3, (c) event 11, and (d) event 14

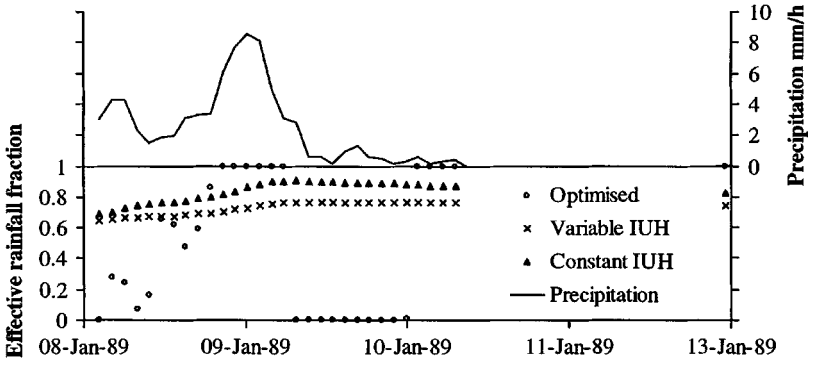

Figure 11. Effective rainfall fraction and precipitation for the validation event 14 in Andrews Watershed 2

identified IUH shape and the event magnitude was not visible in the larger catchments. If such a relationship were to exist then it was masked by other causes, leading to the variability of the IUH between different events.

In the light of the present results an event-magnitude-dependent IUH is necessary to describe the streamflow response to effective rainfall properly in the small catchments (0·18 and 0·63 km^2) of the study. In a rainfall-runoff model application, the event magnitude dependency was characterized in terms of a simple linear

Copyright © 2004 John Wiley & Sons, Ltd.

relationship between the scale parameter of the gamma distribution and the effective rainfall intensity. Comparison of simulation results from two models (involving either a variable- or a constant-IUH scheme) suggests that neglecting the event magnitude dependency of the IUH may lead to underprediction of the highest flows. Large events occur rarely and, therefore, a constant IUH calibrated against the entire record will easily be more representative of smaller, more numerous events, which have a less flashy behaviour.

ACKNOWLEDGEMENTS

This study was funded by the Academy of Finland project 'Predicting impacts of land use changes on catchment hydrological processes' headed by Professor Pertti Vakkilainen, whose support is greatly appreciated. Additional funding was received from the Jenny and Antti Wihuri Foundation, and the Land and Water Technology Foundation. Andrews data sets were provided by the Forest Science Data Bank, a partnership between the Department of Forest Science, Oregon State University, and the US Forest Service Pacific Northwest Research Station, Corvallis, OR. Significant funding for these data was provided by the National Science Foundation Long-Term Ecological Research program (NSF grant numbers BSR-90-11663 and DEB-96-32921). Streamflow and meteorological data from Vantaanjoki basin were provided by the Finnish Environment Institute and Finnish Meteorological Institute respectively. Discussions with Mr Hannu Sirviö and Dr Ari Jolma are acknowledged.

REFERENCES

Aron G, White EL. 1982. Fitting a gamma distribution over a synthetic unit hydrograph. *Water Resources Bulletin* **18**: 95–98.
ASCE. 1996. *Hydrology Handbook*. ASCE Manuals and Reports on Engineering Practice No. 28. ASCE: New York; 784.
Blažková Š. 1992. Empirical study of nonlinearity in direct runoff on a 100 km^2 basin. *Hydrological Sciences Journal* **37**: 347–358.
Blöschl G, Sivapalan M. 1995. Scale issues in hydrological modelling: a review. *Hydrological Processes* **9**: 251–290.
Boufadel MC. 1998. Unit hydrographs derived from the Nash model. *Journal of the American Water Resources Association* **34**: 167–177.
Chen SJ, Singh VP. 1986. Derivation of a new variable instantaneous unit hydrograph. *Journal of Hydrology* **88**: 25–42.
Cheng SJ, Wang RY. 2002. An approach for evaluating the hydrological effects of urbanization and its application. *Hydrological Processes* **16**: 1403–1418.
Ding JY. 1974. Variable unit hydrograph. *Journal of Hydrology* **22**: 53–69.
Duan Q, Sorooshian S, Gupta V. 1992. Effective and efficient global optimization for conceptual rainfall-runoff models. *Water Resources Research* **28**: 1015–1031.
Duband D, Obled C, Rodriguez JY. 1993. Unit hydrograph revisited: an alternative iterative approach to UH and effective precipitation identification. *Journal of Hydrology* **150**: 115–149.
Evans JP, Jakeman AJ. 1998. Development of a simple, catchment-scale rainfall–evapotranspiration–runoff model. *Environmental Modelling & Software* **13**: 385–393.
Garklavs G, Oberg KA. 1986. Effect of rainfall excess calculations on modeled hydrograph accuracy and unit-hydrograph parameters. *Water Resources Bulletin* **22**: 565–572.
Georgakakos AP, Kabouris JC. 1989. A streamflow model using physically-based instantaneous unit hydrographs. *Journal of Hydrology* **111**: 107–131.
Goodrich DC, Lane LJ, Shillito RM, Miller SN, Syed KH, Woolhiser DA. 1997. Linearity of basin response as a function of scale in a semiarid watershed. *Water Resources Research* **33**: 2951–2965.
Gupta VK, Waymire E, Wang CT. 1980. A representation of an instantaneous unit hydrograph from geomorphology. *Water Resources Research* **16**: 855–862.
HWED. 1994. *The program of measures for water protection in River Vantaanjoki watercourse, southern Finland*. A 43, Helsinki Water and Environment District (HWED), National Board of Waters and the Environment, Helsinki (in Finnish).
Jakeman AJ, Hornberger GM. 1993. How much complexity is warranted in a rainfall-runoff model? *Water Resources Research* **29**: 2637–2649.
Jakeman AJ, Littlewood IG, Whitehead PG. 1990. Computation of the instantaneous unit hydrograph and identifiable component flows with application to two small upland catchments. *Journal of Hydrology* **117**: 275–300.
Koivusalo H, Kokkonen T. 2002. Snow processes in a forest clearing and in a coniferous forest. *Journal of Hydrology* **262**: 145–164.
Kokkonen T, Koivusalo H, Karvonen T. 2001. A semi-distributed approach to rainfall-runoff modelling—a case study in a snow affected catchment. *Environmental Modelling & Software* **16**: 481–493.
Lepistö A. 1994. Areas contributing to generation of runoff and nitrate leaching as estimated by empirical isotope methods and TOPMODEL. *Aqua Fennica* **24**: 103–120.
Lepistö A, Kivinen Y. 1997. Effects of climatic change on hydrological patterns of a forested catchment: a physically based modeling approach. *Boreal Environment Research* **2**: 19–31.

Copyright © 2004 John Wiley & Sons, Ltd.

Minshall NE. 1960. Predicting storm runoff on small experimental watersheds. *Journal of the Hydraulics Division. Proceedings of the American Society of Civil Engineers* **86**: 7–38.
Nalbantis I, Obled C, Rodriguez JY. 1995. Unit hydrograph and effective precipitation identification. *Journal of Hydrology* **168**: 127–157.
Nash JE. 1957. *The form of the instantaneous unit hydrograph*. IAHS Publication 45. International Association of Scientific Hydrology: Wallingford; 114–121.
Nash JE. 1959. Systematic determination of unit hydrograph parameters. *Journal of Geophysical Research* **64**: 111–115.
Nash JE, Sutcliffe JV. 1970. River flow forecasting through conceptual models, part I—a discussion of principles. *Journal of Hydrology* **10**: 282–290.
Pilgrim DH, Cordery I. 1992. Flood runoff. In *Handbook of Hydrology*, Maidment DR (ed.). McGraw-Hill: New York; 9·1–9·42.
Robinson JS, Sivapalan M, Snell JD. 1995. On the relative roles of hillslope processes, channel routing, and network geomorphology in the hydrologic response of natural catchments. *Water Resources Research* **31**: 3089–3101.
Rodríguez-Iturbe I. 1993. The geomorphological unit hydrograph. In *Channel Network Hydrology*, Beven K, Kirkby MJ (eds). John Wiley & Sons: Chichester; 42–68.
Rodríguez-Iturbe I, Valdés J. 1979. The geomorphologic structure of hydrologic response. *Water Resources Research* **15**: 1409–1420.
Rodríguez-Iturbe I, Devoto G, Valdés J. 1979. Discharge response analysis and hydrologic similarity: the interrelation between the geomorphologic IUH and the storm characteristics. *Water Resources Research* **15**: 1435–1444.
Rodríguez-Iturbe I, González-Sanabria M, Bras RL. 1982a. A geomorphoclimatic theory of the instantaneous unit hydrograph. *Water Resources Research* **18**: 877–886.
Rodríguez-Iturbe I, González-Sanabria M, Caamaño G. 1982b. On the climatic dependence of the IUH: a rainfall-runoff analysis of the Nash model and the geomorphoclimatic theory. *Water Resources Research* **18**: 887–903.
Rosso R. 1984. Nash model relation to Horton order ratios. *Water Resources Research* **20**: 914–920.
Sherman LK. 1932. Streamflow from rainfall by the unit-hydrograph method. *Engineering News Record* **108**: 501–505.
Sivapalan M, Jothityangkoon C, Menabde M. 2002. Linearity and nonlinearity of basin response as a function of scale: discussion of alternative definitions. *Water Resources Research* **38**: 10·1029/2001WR000482.
Todini E. 1996. The ARNO rainfall-runoff model. *Journal of Hydrology* **175**: 339–382.
Van Cleve K, Martin S. 1991. *Long-Term Ecological Research in the United States*. LTER Network Office: Seattle.
Wang G-T, Singh VP, Yu FX. 1992. A rainfall-runoff model for small watersheds. *Journal of Hydrology* **138**: 97–117.
Young PC. 2001. Data-based mechanistic modelling and validation of rainfall-flow processes. In *Model Validation: Perspectives in Hydrological Science*, Anderson MG, Bates PD (eds). John Wiley: Chichester, 117–161.

Copyright © 2004 John Wiley & Sons, Ltd.